Effect of the Agglomerated State on the Photocatalytic Hydrogen Production with in Situ Agglomeration of Colloidal TiO2 Nanoparticles

ARTICLE *in* THE JOURNAL OF PHYSICAL CHEMISTRY C · DECEMBER 2008

Impact Factor: 4.77 · DOI: 10.1021/jp808541v

THE JOURNAL OF PHYSICAL CHEMISTRY C

Article

Effect of the Agglomerated State on the Photocatalytic Hydrogen Production with in Situ Agglomeration of Colloidal TiO Nanoparticles

Narayanan Lakshminarasimhan, Wooyul Kim, and Wonyong Choi

J. Phys. Chem. C, **2008**, 112 (51), 20451-20457 • DOI: 10.1021/jp808541v • Publication Date (Web): 04 December 2008

Effect of the Agglomerated State on the Photocatalytic Hydrogen Production with in Situ Agglomeration of Colloidal TiO_2 Nanoparticles

Narayanan Lakshminarasimhan, Wooyul Kim, and Wonyong Choi*

School of Environmental Science and Engineering, Pohang University of Science and Technology (POSTECH), Pohang 790-784, Korea

Received: September 26, 2008; Revised Manuscript Received: October 29, 2008

The photocatalytic production of H_2 in aqueous TiO_2 colloid (with methanol as an electron donor) was greatly accelerated by the in situ agglomeration of the colloid although such an agglomeration should reduce the photocatalytic activity in most other cases because of the reduction of the surface area. The in situ agglomeration occurred after an induction period of 3 h and was ascribed to the pH increase which was resulted from the photocatalytic reduction of nitrate (incorporated from the synthetic step of TiO_2 sol) to ammonia. The agglomeration occurred at pH close to the isoelectric point of colloidal TiO_2 which was 6.9 as measured by the ζ-potential. It is proposed that the charge separation is facilitated by electron hopping from particle to particle when TiO_2 nanoparticles are connected with each other within the agglomerates. This behavior was further supported by the photocurrent collection measurement (mediated by the methyl viologen MV^{2+}/MV^{+} redox couple in the colloidal solution), which also showed a rapid increase in the photocurrent after the agglomeration of TiO_2 nanoparticles. When the colloid of TiO_2 was initially coagulated at around pH 6, the production of hydrogen increased linearly with time without showing an induction period and the collected photocurrent showed an immediate increase upon irradiation. To understand the role of the agglomerated state, the colloidal TiO_2 (well-dispersed) and the suspension of commercial TiO_2 (agglomerated) systems were compared and discussed for their photocatalytic behaviors. The present study demonstrates that the degree of agglomeration of TiO_2 nanoparticles is a critical parameter in determining the efficiency of the charge separation and the photocatalytic hydrogen production.

Introduction

Titanium dioxide based photocatalysts find diverse applications such as water/air purification, solar energy conversion including hydrogen production, and self-cleaning coating.[1−4] The particle size, crystallinity, surface area, and morphology of TiO_2 play crucial roles in determining its properties. One of the advantages of a nanoparticulate catalyst is the large specific surface area which provides more surface sites for adsorption and reaction of substrates. However, as for photocatalysis utilizing titania particles it has been often reported that there is no good correlation between the catalyst surface area and the activity since the photocatalytic activity is a complex function of various parameters such as the defect density, surface functionality, and the substrate−surface interaction.[5,6] It has been also reported that an optimum size of TiO_2 nanoparticle is necessary to prevent the undesired bulk and surface recombination of the charge carriers.[7,8] Recently, this group proposed that mesoporous TiO_2 consisting of dense packing of nanoparticles enhances the photocatalytic activity for hydrogen production since the photogenerated charge pairs can be efficiently separated through the interparticle charge transfer within the agglomerate.[9] This suggests that the interconnection among TiO_2 nanoparticles is also an important parameter that affects the photocatalytic activity. However, how the interparticle connectivity and the state of agglomeration of TiO_2 nanoparticles influence the photocatalytic activity has not been well investigated and understood.

Colloidal TiO_2 is a good model system[10−12] in which the effect of agglomeration on the photocatalytic activity can be investigated systematically. The agglomeration of colloidal nanoparticles can be induced by the simple pH adjustment, and the presence of the agglomerated state can be easily detected by naked eyes. In this study, we investigated the effect of colloidal TiO_2 agglomeration on the photocatalytic activity for hydrogen production. During the course of the photocatalytic evolution of hydrogen from UV-illuminated solution (transparent) of colloidal TiO_2 (platinized and with methanol as a hole scavenger), we observed that the evolution of H_2 suddenly increased after an induction period of 3 h, which was coincident with the agglomeration of the colloid. However, such an induction period of hydrogen production was not observed in the illuminated suspension (turbid) of TiO_2 that consisted of agglomerated nanoparticles. This observation motivated us to understand this peculiar behavior of the colloidal TiO_2 system. The role of in situ agglomeration of colloidal TiO_2 nanoparticles in enhancing the photocatalytic production of hydrogen was investigated and discussed to propose that the photocatalysis is accelerated through the interparticle charge transfer within the TiO_2 agglomerate.

Experimental Section

Synthesis and Characterization. The colloidal TiO_2 nanoparticles were synthesized according to the procedure described elsewhere which involves the hydrolysis of titanium tetraisopropoxide (TTIP) in the presence of nitric acid.[9] In a typical synthesis, a mixture of 30 mL of TTIP (Junsei, 98%) and 5 mL of 2-propanol (Junsei, 99.5%) was added to 180 mL of distilled

* Corresponding author. Fax: +82-54-279-8299. E-mail: wchoi@postech.edu.

10.1021/jp808541v CCC: $40.75
Published on Web 12/04/2008

water, and then 2 mL of concentrated nitric acid (60% solution) was added. The mixture was heated at 80 °C for 8 h, and then the solvent was evaporated under low pressure using a rotatory evaporator to get the final powder product.

The powder sample contained nitrate residue originated from nitric acid used in the synthetic procedure. Fourier transform infrared (FT-IR) spectroscopic technique identified the surface nitrate species present on the TiO_2 sample using the KBr pellet technique with a Bomem (ABB Bomem, MB series) instrument. The presence of nitrate residue was confirmed by its stretching vibration at 1385 cm^{-1} in the FT-IR spectrum (see the Supporting Information, Figure S1).[13] When the TiO_2 powder was redissolved in distilled water, it yielded pH = 3.0 and $[NO_3^-]$ = 1.2 mM at $[TiO_2]$ = 1.0 g/L. When needed, the colloidal TiO_2 was agglomerated by adjusting the solution pH to 6.0 with 0.1 M NaOH. In order to understand the role of agglomeration, similar experiments were carried out with commercial TiO_2 powder (Hombikat, UV-100) that consisted of agglomerated nanoparticles. For this purpose, Hombikat (HBK) powder was suspended and stirred in aqueous nitric acid solution for 8 h and then dried using a rotatory evaporator. That is, the commercial TiO_2 was treated with nitric acid under the identical condition to that of the colloidal TiO_2 synthesis. The photocatalytic activity of colloidal TiO_2 was compared with the nitric acid treated HBK sample (HBK/HNO_3) under the identical experimental condition.

Powder X-ray diffraction (XRD) was used for the crystalline phase analysis using Cu Kα radiation (MAC Science Co., M18XHF). The X-ray diffractogram of the synthesized colloidal TiO_2 sample showed broad reflections which were indexed based on the anatase phase of TiO_2 (Supporting Information, Figure S1). The crystallite size of 6.8 nm was obtained using the Scherrer formula.[14] The surface area was measured using a Micromeritics ASAP 2000 instrument and analyzed according to the Brunauer−Emmett−Teller (BET) method. The measured BET surface area was 163 $m^2\ g^{-1}$. The UV−vis absorption spectra of the colloidal solution were recorded at different pH values using a spectrophotometer (Agilent 8453). The ζ-potential and hydrodynamic particle size of colloidal TiO_2 (0.1 g/L) were measured as a function of pH using an electrophoretic light scattering spectrophotometer (ELS 8000, Otsuka). The solution pH was adjusted with HNO_3 and NaOH solutions.

Photocatalytic Activity Measurements for Hydrogen Production. The TiO_2 powder obtained from the above procedure was redissolved in aqueous solution to make a transparent colloidal solution (pH 3.0 with $[TiO_2]$ = 1.0 g/L), and then methanol (10% v/v) was added as an electron donor. In the resulting colloidal solution of TiO_2, chloroplatinic acid was added and platinum (0.1 wt %) was reductively photodeposited on the surface of TiO_2 as a cocatalyst of hydrogen production.[15] After photodeposition of Pt for 30 min, the reactor was sealed with rubber septum and purged with N_2 gas for 45 min before initiating the UV irradiation for H_2 evolution. The initial pH of the colloidal solution was typically 3.0 ± 0.1. The slurry of HBK/HNO_3 was also photoplatinized and purged with nitrogen prior to irradiation in the same way.

The reactor used was a Pyrex bottle with a total solution volume of 30 mL. A 450 W Xe arc lamp (Oriel) was used as the light source, and the light passed through a 10 cm IR water filter and a UV cutoff filter ($\lambda > 300$ nm). The evolved H_2 was sampled from the reactor headspace using a gas-tight syringe and analyzed by a gas chromatograph (GC, HP6890N) with a thermal conductivity detector using N_2 as carrier gas. The photonic efficiency ξ for H_2 production was calculated as ξ = (2 × rate of H_2 evolution)/(incident light intensity). The incident light intensity was measured to be 2.26×10^{-3} einstein min^{-1} L^{-1} by ferrioxalate actinometry.[16] Along with the production of H_2, the nitrates (NO_3^-) contained in the TiO_2 sol were concurrently reduced to ammonium ions (NH_4^+), which was followed using an ion chromatograph (IC, Dionex DX-120). The sample aliquots for IC analysis were collected under similar conditions to that of the H_2 evolution photoreaction, then the pH was adjusted to 6.0 with NaOH solution to coagulate colloidal TiO_2 particles that were removed through a 0.45 μm PTFE filter prior to the IC analysis.

Photoelectrochemical Measurements. The electron shuttle-mediated photocurrent collection from the illuminated TiO_2 colloidal solution was carried out using a three-electrode assembly as described previously.[17] A Pt plate (1 × 1 cm^2), a graphite rod, and a standard calomel electrode (SCE) were used as a working, a counter, and a reference electrode, respectively. Methyl viologen (MV^{2+}) (1 mM) was used as the electron shuttle, KNO_3 (0.1 M) as the electrolyte, and CH_3OH (10% v/v) as the hole scavenger as in the H_2 evolution experiment. N_2 gas was continuously purged through the colloidal solution before and during the irradiation. The colloidal solution was magnetically stirred during the UV irradiation ($\lambda > 300$ nm). The photocurrents were collected by applying a potential (+0.1 V vs SCE) to the Pt working electrode using a potentiostat (EG&G 263A2) that was connected to a computer.

Photocatalytic Activity Measurements for the Conversion of Pollutants. The photocatalytic activity of the colloidal TiO_2 (platinized) was also tested for comparison with the production of hydrogen. Two different sols, one at pH 3 (colloidal) and the other at pH 6 (agglomerated), were compared. The following chemicals were used as test substrates: 4-chlorophenol (4-CP, Sigma), tetramethylammonium hydroxide (TMA, Aldrich), and sodium dichromate (Cr(VI), Aldrich). The typical concentration of TiO_2 colloid was 0.5 g/L. The concentrations of 4-CP, TMA, and Cr(VI) were 100, 100, and 200 μM, respectively. The aqueous colloid was stirred for 20 min to allow the equilibrium adsorption of substrates on TiO_2. A 300 W Xe arc lamp (Oriel) combined with a 10 cm IR water filter and cutoff filters ($\lambda >$ 300 nm for TMA and Cr(VI) and $\lambda > 320$ nm for 4-CP) was used as a light source. A 30 mL Pyrex reactor was open to the ambient air and stirred magnetically during irradiation. Sample aliquots were withdrawn by a 1 mL syringe intermittently during the photoreaction, and the TiO_2 colloid was coagulated and filtered before the analysis. The concentration of 4-CP was quantified using a high-performance liquid chromatograph (HPLC, Agilent 1100 series) equipped with a diode array detector and a ZORBAX 300SB C18 column (4.6 mm × 150 mm). The eluent consisted of 0.1% phosphoric acid solution and acetonitrile (80:20 by volume). The analysis of TMA was performed by IC. The concentration of Cr(VI) was analyzed using a colorimetric method that uses 1,5-diphenylcarbazide (DPC) reagent.[18] The color change was monitored at 540 nm ($\varepsilon = 4 \times 10^4$ L g^{-1} cm^{-1}) using a UV−vis spectrophotometer (Shimadzu, UV-2401 PC).

Results and Discussion

Hydrogen Production Behavior in Illuminated TiO_2 Colloid. The photocatalytic H_2 evolution in the aqueous Pt/TiO_2 colloid was tested under UV light irradiation. The time course of H_2 evolution is shown in Figure 1a. The H_2 evolution was initially negligible but abruptly increased after an induction period of 3 h (ξ = 1.3% during 3−8 h). It should be noted that the acceleration of hydrogen production after 3 h was coincident

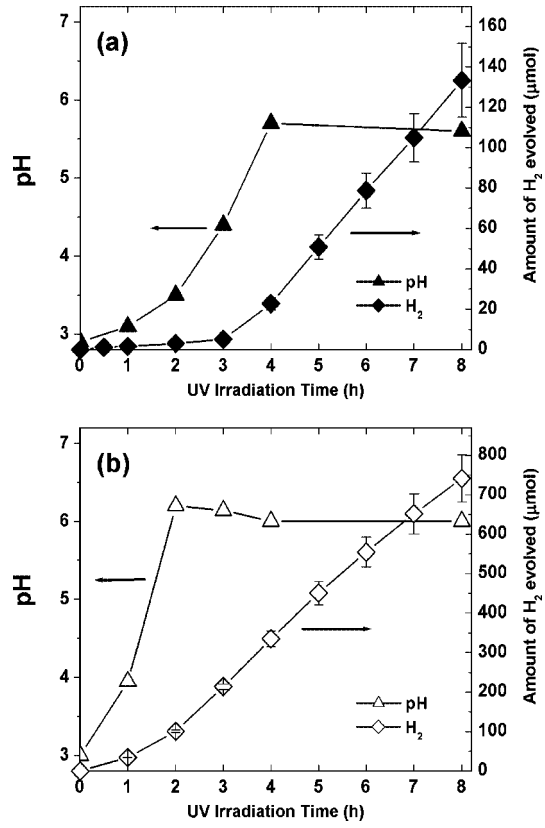

Figure 1. Time course of H_2 evolution and variation of pH in (a) colloidal TiO_2 and (b) HBK/HNO_3 suspension: [TiO_2] = 1 g/L (with 0.1 wt % Pt); 10% (v/v) CH_3OH in water; $\lambda > 300$ nm.

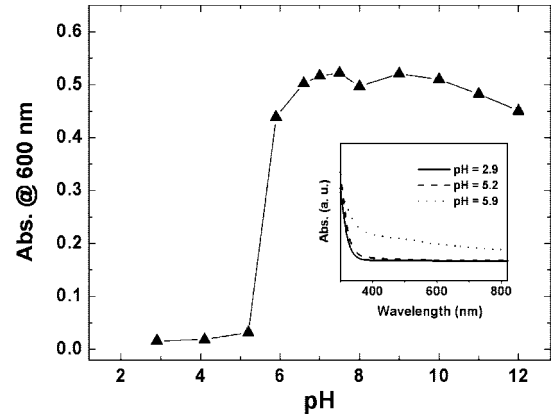

Figure 2. Variation in the absorbance (at 600 nm) of the colloidal TiO_2 as a function of pH; the inset showing the UV−vis absorption spectra of colloidal TiO_2 at selected pH.

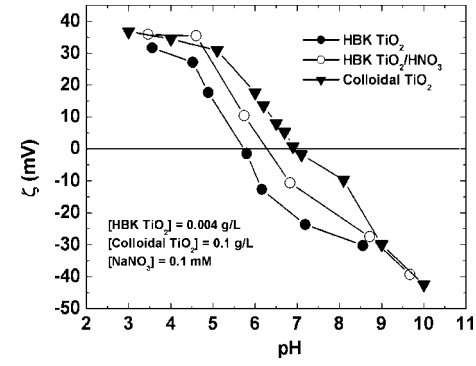

Figure 3. pH-dependent ζ-potential of colloidal TiO_2, HBK, and HBK/HNO_3 suspensions in the presence of $NaNO_3$ (0.1 mM); pH adjusted with NaOH and HNO_3 solutions.

with the agglomeration of the colloids. The agglomerated particles were observed visibly in the solution, whereas the original sol was nearly transparent in a well-dispersed state (Supporting Information, Figure S2). The hydrodynamic particle size of colloidal TiO_2 measured by light scattering increased drastically from 41 nm at pH 3.0 (initial colloid) to 4.5 μm at pH 6.0 (after coagulation) (Supporting Information, Figure S3). The agglomeration seemed to be induced by the in situ pH increase during the irradiation. The pH of the colloidal solution was measured at different stages of irradiation (1, 2, 3, 4, and 8 h) and is shown in Figure 1a along with the time profile of hydrogen production. Starting from 3.0 ± 0.1, the pH increased with the irradiation time and the rate of the pH increase was markedly accelerated around 3 h, which was synchronous with the colloid agglomeration. The relation between pH and the agglomeration of colloidal TiO_2 is shown in Figure 2. The absorbance of the colloidal TiO_2 solution at 600 nm, which is an indicator of turbidity (light scattering by agglomerates), abruptly jumped when the pH increased from 5.2 to 5.9. This pH range was reached after around 3.5 h of irradiation according to Figure 1a, which coincides with the agglomeration. This clearly indicates that the onset of the agglomeration of TiO_2 colloid during the irradiation should be ascribed to the in situ pH rise during photocatalysis.

To compare with the colloidal TiO_2 (Figure 1a), the slurry of HBK/HNO_3 was also tested for the photocatalytic hydrogen production under the identical experimental condition. The turbid slurry of HBK/HNO_3 consists of highly agglomerated nanoparticles, whereas the transparent TiO_2 colloid is composed of well-dispersed nanoparticles. Figure 1b shows the time profile of hydrogen evolution and the accompanying pH change in the UV-illuminated slurry of platinized catalyst of HBK/HNO_3. No drastic change in the rate of hydrogen production was observed throughout the irradiation in the slurry system, whereas a sudden increase in the hydrogen production rate was observed during the irradiation in the colloidal TiO_2 system. Although the dispersiveness of colloidal TiO_2 should be sensitive to pH change, that of commercial TiO_2 particles in the slurry phase is less affected by pH because they are already agglomerated from the beginning. This implies that the sudden acceleration of hydrogen production in the colloidal system may be related with the appearance of the agglomerated state. Although more incident light should be scattered out in the agglomerated state with less light absorbed by the TiO_2 colloid, H_2 production was enhanced in the agglomerated state. This implies that the agglomeration effect outweighs the scattering-reduced light intensity.

In Situ pH Change and Agglomeration in Colloidal TiO_2. The pH-induced agglomeration of colloids is a classical phenomenon related with the surface chemistry of metal oxides. In order to find the isoelectric point (IEP) of colloidal TiO_2, the ζ-potential was measured as a function of pH (Figure 3). The point of zero ζ-potential is taken as the IEP, and the observed value is 6.9 in this case. This value is higher than the point of zero charge (PZC) (3.0−6.0) that has been normally reported for TiO_2.[19] In general, IEP is different from PZC when there are specifically adsorbed ions on the particle surface.[20] Under this situation the PZC and IEP shift in the opposite direction from IEP_0 (= PZC_0; obtained in the absence of specific ion adsorption). Thus in the present study, the higher IEP of colloidal TiO_2 should be ascribed to the adsorption of NO_3^- ions. This is further confirmed from the ζ-potential measurements done with the commercial TiO_2 sample (pure HBK and

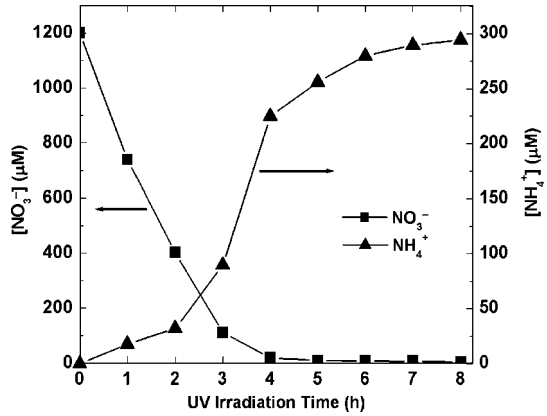

Figure 4. Time profiles of the removal of NO_3^- and the production of NH_4^+ along with the H_2 evolution reaction in colloidal TiO_2; the experimental conditions were similar to those in Figure 1.

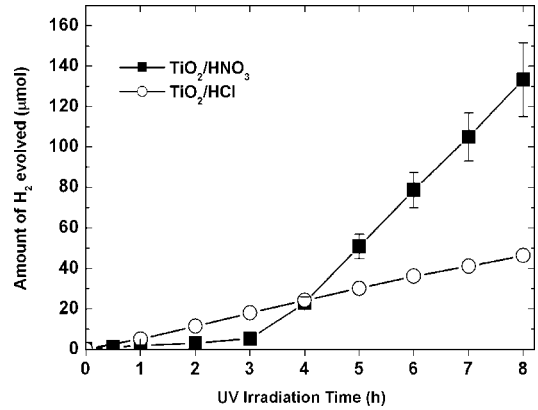

Figure 5. Time course of H_2 evolution in colloidal TiO_2 synthesized using HNO_3 or HCl; the experimental conditions were similar to those in Figure 1. The uncertainty with TiO_2/HCl is within the size of the symbol.

HBK/HNO_3) as shown in Figure 3. In this case, the presence of HNO_3 shifted IEP to a higher pH value. As the pH approaches closer to IEP, the vanishing surface charge allows the particles to come closer and coagulate through van der Waals attraction.[21] The agglomeration should be possible when the pH is within one unit above or below IEP of TiO_2.

The rapid increase of pH during the photocatalytic hydrogen evolution was observed in both colloidal TiO_2 and the slurry HBK/HNO_3 system (Figure 1). The UV-induced pH change in the colloidal TiO_2 seems to be related with the photocatalytic conversion of residual nitric acid that was added in the synthetic step. It has been reported that NO_3^- can be photocatalytically reduced to NH_3 on Pt/TiO_2 in the presence of methanol (electron donor) under anoxic condition.[22]

$$NO_3^- + 9H^+ + 8e^- \rightarrow NH_3 + 3H_2O \quad (1)$$

The reduction of NO_3^- can also proceed in the presence of H_2 over Pt metal surface in the dark. Therefore, it may be possible that the photocatalytically produced H_2 over Pt/TiO_2 is consumed in situ for reducing nitrates.[22] As a result of this reductive conversion, the solution pH should increase.

Figure 4 confirms that nitrates were indeed photocatalytically converted into ammonium ions in colloidal TiO_2. In the colloidal TiO_2 system, the concentration of NO_3^- showed a drastic decrease during the initial 3 h, but the accompanying production of NH_4^+ was sluggish during the initial 2 h. A sharp increase was observed in [NH_4^+] between 3 and 4 h during which the solution pH also rose sharply to reach a saturation value (see Figure 1a). Thus, the formation of NH_4^+ from the reduction of surface NO_3^- ions should be responsible for the increase in solution pH and also for the agglomeration of TiO_2 colloid. As the pH approached 5.6−5.9 within the limit of one unit below IEP, the ζ-potential fell below 20 mV (from 37 mV at pH 3) with weakening of the electrostatic repulsive force, and consequently, the originally well-dispersed colloidal TiO_2 started coagulating.[21] It is noted that the concentrations of NO_3^- and NH_4^+ were nearly equal (100 μM) at 3 h of photocatalytic reaction. This indicates that the residual nitric acid is neutralized with an equal amount of in situ generated NH_3 resulting in the loss of electrical double layer, and hence the particles started coagulating. That is, the agglomeration of colloidal TiO_2 after an induction period was caused by the in situ pH increase, which was resulted from the photocatalytic conversion of nitrates. Incidentally, the photocatalytic conversion of NO_3^- into NH_4^+ was not quantitative (no N-balance matched) and the formation of intermediate NO_2^- was not observed at all. This implies that there should be other missing products such as N_2. The photocatalytic conversion of NH_3 into N_2 on Pt/TiO_2 has been reported in the literature (reaction 2).[23,24] The in situ generated H_2 may also react with NO_3^- to generate N_2 on Pt/TiO_2 in the dark (reaction 3).[25]

$$2NH_3 + 6h_{vb}^+ \rightarrow N_2 + 6H^+ \quad (2)$$

$$2NO_3^- + 5H_2 \rightarrow 4H_2O + N_2 + 2OH^- \quad (3)$$

In order to confirm the role of nitrate conversion in the overall photocatalytic process of hydrogen production, a control experiment was carried out using another colloidal TiO_2 synthesized through a similar procedure using HCl instead of HNO_3. The result is shown in Figure 5. In this control case (TiO_2/HCl), there was no agglomeration of colloidal particles even after 12 h of irradiation and the photocatalytic H_2 production increases linearly with time without exhibiting any induction period (ξ = 0.30% during 0−5 h). There was little pH change in the irradiated colloidal solution of TiO_2/HCl: the initial and final pH values were 2.84 and 2.90 (after 8 h), respectively. This assures that the photocatalytic conversion of nitrates induces the pH increase, which subsequently causes the colloid agglomeration with accelerating the production of hydrogen in the colloidal TiO_2 system.

An alternative explanation for the acceleration of hydrogen generation after an induction period may be related with the preferential reduction of NO_3^- over H_2 production during the induction period. Nitrates should compete for conduction band electrons with protons according to reaction 1 and therefore should inhibit the production of hydrogen. Comparison between Figure 1a and Figure 4 shows that the production of hydrogen started only after most nitrates were removed in the colloidal TiO_2. Since the point of nitrate depletion, the onset of the rapid pH increase, and the agglomeration of TiO_2 colloid all occur concurrently, it is difficult to judge whether the acceleration of hydrogen production was induced by the depletion of competing nitrates or the colloidal agglomeration. To separate the effect of nitrate depletion from that of the colloidal agglomeration, the photocatalytic hydrogen production was investigated in HBK TiO_2 slurry with and without HNO_3. Since this commercial TiO_2 sample is highly agglomerated from the beginning, the agglomeration effect on the hydrogen production should be minimal. Figure 6 shows that the appearance of the induction period was not as obvious as in the case of colloidal TiO_2 system although the rate of hydrogen production was retarded by the

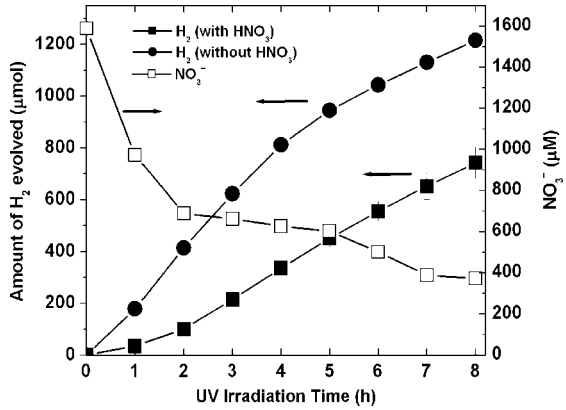

Figure 6. Time course of H_2 evolution with commercial HBK TiO_2 with and without HNO_3: $[TiO_2] = 1$ g/L (with 0.1 wt % Pt); 10% (v/v) CH_3OH in water; pH_i 3.0 (with HNO_3) and pH_i 5.7 (without HNO_3); $\lambda > 300$ nm. The time course of NO_3^- removal is also shown.

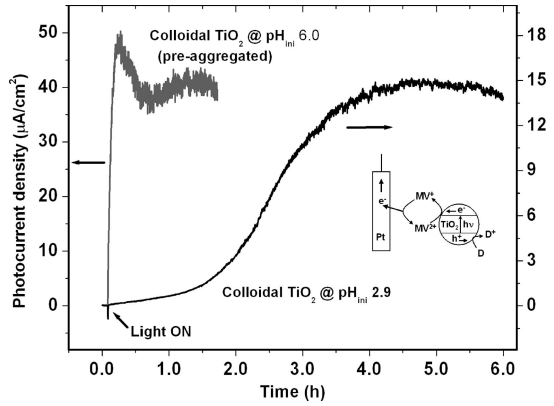

Figure 7. Time profiles of the photocurrent collected by MV^{2+}/MV^+ electron shuttle in N_2-saturated colloidal TiO_2 at pH_{ini} 2.9 (well-dispersed) and 6.0 (agglomerated); $[TiO_2] = 1$ g/L (without Pt); 10% (v/v) CH_3OH in water; $[MV^{2+}] = 1$ mM; $[KNO_3] = 0.1$ M; applied potential $= +0.1$ V (vs SCE); $\lambda > 300$ nm.

presence of HNO_3. The profile of nitrate removal is also shown along with the hydrogen production profile. The nitrate removal was fast in the initial period of 2 h but was markedly decelerated in the later stage. Throughout the irradiation period, the hydrogen production rate was significant even in the presence of remaining nitric acid (>300 μM). Although the photocatalytic reduction of nitrates decreases the production rate of hydrogen, it does not seem to be a main reason for the induction period after which the hydrogen production is abruptly accelerated in the colloidal TiO_2.

Role of the Agglomerated State in Photocatalytic Hydrogen Production. On the basis of the above arguments, it is logical to propose that the synchronous hydrogen production and colloid agglomeration should be directly related. To confirm this, we measured the photocurrent (Figure 7) collected in the TiO_2 colloid using MV^{2+}/MV^+ as a redox shuttle as a function of the UV irradiation time. In this case, bare TiO_2 colloid (without Pt deposit) was used since MV^+ could be reoxidized on Pt sites. The time profile of the collected photocurrent is very similar to that of H_2 production. Like the hydrogen generation profile shown in Figure 1a, the photocurrent was very low during the initial period (with pH_{ini} 2.9) and then rapidly increased upon agglomeration to reach a saturation value. However, when the TiO_2 colloid was initially coagulated at pH 6.0 (by adjusting the pH with NaOH solution), the photocurrent immediately increased upon irradiation without showing an induction period. This clearly indicates that the efficiency of

SCHEME 1: Schematic Illustration Showing the Well-Dispersed Colloidal TiO_2 Nanoparticles at pH 2.9 and Agglomerated TiO_2 Nanoparticles (pH 5.9) with Higher H_2 Production Activity Due to Interparticle Charge Transport

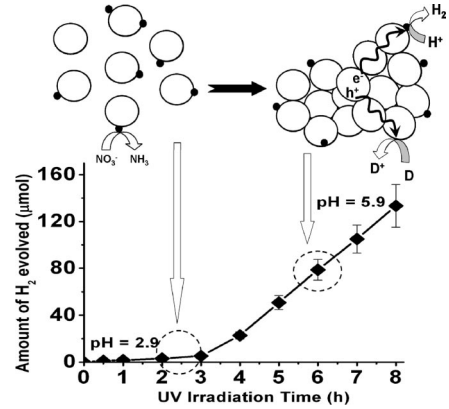

the photoinduced electron transfer increases as a result of the colloid agglomeration. The agglomerated state brings TiO_2 nanoparticles in close contact with each other through the grain boundaries, and the photogenerated charge carriers in the agglomerate should have a lower probability of recombination because the electron and the hole can migrate to an adjacent particle hopping through the grain boundary as depicted in Scheme 1. This is similar to the energy transfer in agglomerated TiO_2 particles as previously explained by the antenna mechanism in which the energy absorbed by one TiO_2 particle is transferred from particle to particle to a remote particle onto which the target molecule is adsorbed.[26] The same antenna effect has recently been employed in explaining the formation of Ag clusters during photodeposition over colloidal TiO_2.[27] In this case, the photoinduced electron transfer from a TiO_2 nanoparticle to a remote nanoparticle occurs through a self-assembled TiO_2 aggregate. Similarly, in the present study, the electron transport to the remote Pt site becomes efficient in the agglomerate rather than in well-dispersed colloidal TiO_2 nanoparticles. Therefore, the sudden acceleration of the hydrogen production rate in the colloidal TiO_2 system is ascribed to the enhanced charge separation within the agglomerates. Incidentally, it is noted that the photocurrent obtained at pH 6 (after saturation) is much higher than that obtained at pH 3 because of the higher electrochemical driving force for the reduction of MV^{2+} [$E^0(MV^{2+}/MV^+) = -0.445$ V_{NHE}]. The TiO_2 conduction band edge potential shifts to more negative value with increasing pH (60 mV/pH)[28] according to the Nernstian behavior and has a higher driving force to reduce MV^{2+}. However, this shift in the TiO_2 conduction band edge potential is not responsible for the enhanced H_2 production since H^+/H_2 reduction potential also shifts in a similar way (60 mV/pH) due to its dependence on the proton concentration.[29]

If the agglomerated state is responsible for the enhancement in the H_2 production after the observed induction period, then one would expect a lower production of H_2 if the agglomeration is broken up. To test this, we readjusted the pH with $HClO_4$ to the original value of 3.0 at the point of agglomeration onset (i.e., after 3 h when most nitrates were used up) and then sonicated the solution to break the agglomerates apart. Figure 8a compares the H_2 production in the deagglomerated colloid with that in the original agglomerated colloid. The rate of H_2 production was much lower ($\xi = 0.36\%$) with the deagglomerated colloid even though the nitrates were almost depleted in

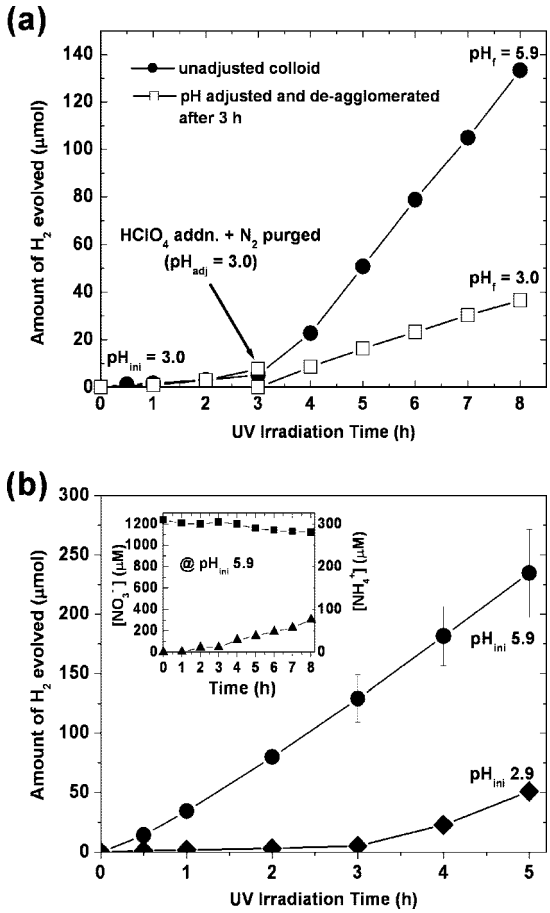

Figure 8. (a) H_2 evolution after the deagglomeration of the TiO_2 colloid by readjusting the pH to 3.0 with $HClO_4$ followed by sonication is much lower than that in the original agglomerated TiO_2 colloid. (b) Comparison of time course of H_2 evolution between initially agglomerated TiO_2 colloid at pH_{ini} 5.9 and the original colloid at pH_{ini} 2.9. The experimental conditions were similar to those in Figure 1. The inset in panel b shows the concurrent conversion of NO_3^- to NH_4^+ at pH_{ini} 5.9.

this case (see Figure 4). This confirms that the rapid enhancement in the H_2 production with colloidal TiO_2 is directly related with the agglomerated state of the nanoparticles.

To further investigate the role of TiO_2 colloid agglomeration, the photocatalytic hydrogen production was also carried out using the initially agglomerated TiO_2 at pH 5.9 ± 0.1. In Figure 8b, the time course of H_2 evolution obtained with the initially agglomerated TiO_2 is compared with that obtained with colloidal TiO_2 at pH 2.9 ± 0.1. The H_2 evolution at pH 5.9 linearly increased ($\xi = 2.3\%$) without showing an induction period. It should be also noted that the photocatalytic conversion of nitrates to ammonium ions is insignificant (inset in Figure 8b) with the initially agglomerated TiO_2. This suggests that the surface chemistry of TiO_2 colloid plays a crucial role in the observed photocatalytic processes. The photocatalytic reduction of nitrates is highly favored at pH 3 and hindered at pH 6, whereas the opposite trend was observed with the photocatalytic hydrogen production. The NO_3^- species should be close to the TiO_2 surface for its conversion to NH_4^+, whereas at pH = 6.0, the NO_3^- species are removed from the surface region into the diffuse layer retarding its reduction. In the TiO_2 colloid containing nitric acid, the initial reaction occurring in the acidic region mainly involves the photocatalytic conversion of nitrates to ammonium ions. This process is essentially a *photocatalytic titration* in which the residual nitric acid is neutralized by the

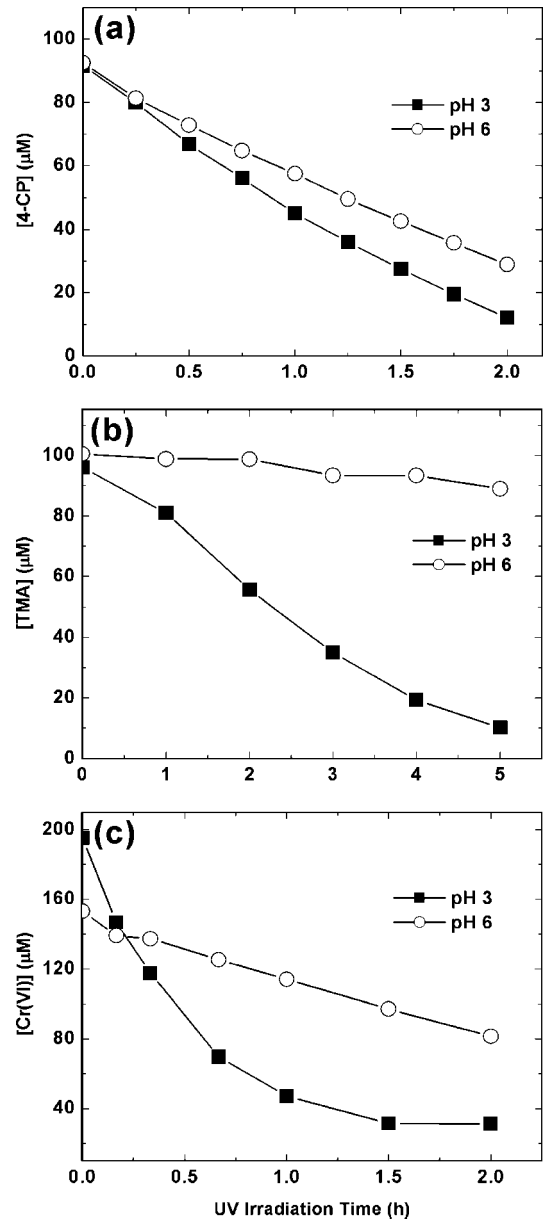

Figure 9. Photocatalytic conversion of (a) 4-CP, (b) TMA, and (c) Cr(VI) with colloidal TiO_2 at pH 3 and 6. [4-CP] = [TMA] = 100 μM; [Cr(VI)] = 200 μM; [TiO_2] = 0.5 g/L. NaOH (0.1 M) solution was used to adjust the pH to 6 to agglomerate TiO_2.

in situ generated ammonia. When the nitric acid is depleted as a result of the photocatalytic reaction, the neutralization is completed with thinning the electrical double layer and the colloid agglomeration sets in. However, this kind of photoinduced agglomeration process does not occur when the nitric acid is absent. In the absence of the agglomerated state, the photocatalytic hydrogen production is inefficient (Figure 8a).

Whether the TiO_2 agglomeration-induced acceleration of photocatalysis is observed with other photocatalytic processes is an interesting question. If the photoinduced charge separation is enhanced with the formation of TiO_2 agglomerates, the photocatalysis should be enhanced in general regardless of the type of photocatalytic processes. Figure 9 compares the photocatalytic conversions of 4-CP, TMA, and Cr(VI) between the TiO_2 colloidal systems at pH 3 (well-dispersed state) and pH 6 (agglomerated state). The conversion of 4-CP and TMA is oxidative, whereas that of Cr(VI) is reductive ($Cr^{6+} \rightarrow Cr^{3+}$). For all cases, the photocatalytic conversion rate was retarded

with the agglomerated colloid (at pH 6), which is contrary to the case of hydrogen production (compare Figure 8 vs Figure 9). Since the pH dependence of the photocatalytic conversion is highly substrate-specific, the reduced photocatalytic activity at pH 6 cannot be ascribed solely to the agglomeration. Nevertheless, the observation that the three substrates (*of very different kind*) all showed the reduced activity at pH 6 indicates that the agglomeration-enhanced activity cannot be generally applied to the cases other than H_2 production. The positive agglomeration effect on the photocatalysis seems to be unique to the hydrogen production system. Since the colloidal agglomeration accompanies the reduction of the available surface area, the photocatalytic conversion of substrates should be limited by the reduced surface area. However, the exact quantification of the change in the reactive surface area of nanoparticles due to agglomeration in the aqueous suspension still remains unknown.[30] The mass transfer of substrates to the active surface sites should be also highly hindered by the agglomerate formation. Therefore, the reduction in the surface area seems to outweigh the agglomeration-enhanced charge separation in the above cases. As for the photocatalytic hydrogen production system in which the substrate is the solvent itself (water and protons), the surface area reduction upon agglomeration should have an insignificant effect because the mass transfer of substrate (water) to the surface is not affected by the agglomeration.

Conclusions

The colloidal TiO_2 that contains nitric acid exhibited an interesting behavior in that the photocatalytic production of hydrogen was suddenly accelerated after an induction period. The production of hydrogen was synchronous with the agglomeration of TiO_2 colloid. The agglomeration was a result of in situ pH increase associated with the simultaneous reduction of nitrate into ammonia, and such an irradiation-induced agglomeration was not observed at all with TiO_2 colloid that contains hydrochloric acid instead of nitric acid. Also, the initially agglomerated TiO_2 colloid (at pH 5.9 ± 0.1) showed a linear increase in H_2 production without exhibiting an induction period. The photocurrents data collected in the TiO_2 colloid are consistent with the photocatalytic behavior. It is proposed that the photocatalytic production of hydrogen is efficient only when colloidal nanoparticles are agglomerated because the charge pair separation is facilitated by the interparticle charge transfer within the agglomerates. However, it should be noted that the agglomeration-induced acceleration in photocatalysis is uniquely observed only with the production of hydrogen but not with other photocatalytic conversions of organic and inorganic substrates. In conclusion, this study proposes that the agglomeration of TiO_2 nanoparticles is a critical factor in obtaining a higher efficiency of the photocatalytic hydrogen production. Although many parameters related with photocatalysts for hydrogen production have been investigated, the importance of the agglomerated state of nanoparticles has not been recognized. This new factor should be taken into account when the photocatalyst for hydrogen production is developed.

Acknowledgment. This work was supported by a KOSEF Grant funded by the Korea government (MEST) (No. R0A-2008-000-20068-0), the KOSEF EPB center (Grant No. R11-2008-052-02002), and the Brain Korea 21 program.

Supporting Information Available: FT-IR spectrum, powder XRD pattern, photographs of colloidal TiO_2, and hydrodynamic particle size of colloidal TiO_2. This material is available free of charge via the Internet at http://pubs.acs.org.

References and Notes

(1) Hoffmann, M. R.; Martin, S. T.; Choi, W.; Bahnemann, D. W. *Chem. Rev.* **1995**, *95*, 69.
(2) Fujishima, A.; Rao, T. N.; Tryk, D. A. *J. Photochem. Photobiol., C* **2000**, *1*, 1.
(3) Duonghong, D.; Borgarello, E.; Grätzel, M. *J. Am. Chem. Soc.* **1981**, *103*, 4685.
(4) Abe, R.; Sayama, K.; Arakawa, H. *Chem. Phys. Lett.* **2003**, *371*, 360.
(5) Yurdakal, S.; Loddo, V.; Ferrer, B. B.; Palmisano, G.; Augugliaro, V.; Farreras, J. G.; Palmisano, L. *Ind. Eng. Chem. Res.* **2007**, *46*, 7620.
(6) Ryu, J.; Choi, W. *Environ. Sci. Technol.* **2008**, *42*, 294.
(7) Zhang, Z.; Wang, C.-C.; Zakaria, R.; Ying, J. Y. *J. Phys. Chem. B* **1998**, *102*, 10871.
(8) Baiju, K. V.; Shukla, S.; Sandhya, K. S.; James, J.; Warrier, K. G. K. *J. Phys. Chem. C* **2007**, *111*, 7612.
(9) Lakshminarasimhan, N.; Bae, E.; Choi, W. *J. Phys. Chem. C* **2007**, *111*, 15244.
(10) Duonghong, D.; Ramsden, J.; Grätzel, M. *J. Am. Chem. Soc.* **1982**, *104*, 2977.
(11) Rothenberger, G.; Moser, J.; Grätzel, M.; Serpone, N.; Sharma, D. K. *J. Am. Chem. Soc.* **1985**, *107*, 8054.
(12) Brown, G. T.; Darwent, J. R. *J. Chem. Soc., Chem. Commun.* **1985**, 98.
(13) Nakamoto, K. *Infrared and Raman Spectra of Inorganic and Coordination Compounds*, 5th ed.; John Wiley & Sons, Inc.: New York, 1997.
(14) West, A. R. *Solid State Chemistry and Its Applications*; John Wiley & Sons Ltd.: Singapore, 1989.
(15) Kraeutler, B.; Bard, A. J. *J. Am. Chem. Soc.* **1978**, *100*, 4317.
(16) Hatchard, C. G.; Parker, C. A. *Proc. R. Soc. London* **1956**, *A235*, 518.
(17) Park, H.; Choi, W. *J. Phys. Chem. B* **2003**, *107*, 3885.
(18) Clesceri, L. S., Greenberg, A. E., Eaton, A. D., Eds. *Standard Methods for the Examination of Water and Wastewater*; APHA: Washington, DC, 1998.
(19) Parks, G. A. *Chem. Rev.* **1965**, *65*, 177.
(20) Cornell, R. M.; Posner, A. M.; Quirk, J. P. *J. Colloid Interface Sci.* **1975**, *53*, 6.
(21) Guzman, K. A. D.; Finnegan, M. P.; Banfield, J. F. *Environ. Sci. Technol.* **2006**, *40*, 7688.
(22) Kudo, A.; Domen, K.; Maruya, K.; Onishi, T. *Chem. Lett.* **1987**, *16*, 1019.
(23) Lee, J.; Park, H.; Choi, W. *Environ. Sci. Technol.* **2002**, *36*, 5462.
(24) Kato, H.; Kudo, A. *Phys. Chem. Chem. Phys.* **2002**, *4*, 2833.
(25) Deganello, F.; Liotta, L. F.; Macaluso, A.; Venezia, A. M.; Deganello, G. *Appl. Catal., B* **2000**, *24*, 265.
(26) Wang, C.-Y.; Pagel, R.; Dohrmann, J. K.; Bahnemann, D.W. *C. R. Chim.* **2006**, *9*, 761.
(27) Friedmann, D.; Hansing, H.; Bahnemann, D. *Z. Phys. Chem.* **2007**, *221*, 329.
(28) Ward, M. D.; White, J. R.; Bard, A. J. *J. Am. Chem. Soc.* **1983**, *105*, 27.
(29) Memming, R. *Semiconductor Electrochemistry*; Wiley-VCH: Germany, 2001; p 56.
(30) Pettibone, J. M.; Cwiertny, D. M.; Scherer, M.; Grassian, V. H. *Langmuir* **2008**, *24*, 6659.

JP808541V